ANTICANCER RESEARCH *41*: 645-660 (2021)
doi:10.21873/anticanres.14816

Urokinase-type Plasminogen Activator Is a Therapeutic Target for Overcoming Sorafenib Resistance in Hepatoma Cells

MAMI OSAWA[1], YASUNOBU MATSUDA[2], YOSHIAKI KINOSHITA[3] and TOSHIFUMI WAKAI[1]

[1]Division of Digestive and General Surgery, Niigata University Graduate School of Medical and Dental Sciences, Niigata, Japan;
[2]Department of Medical Technology, Niigata University Graduate School of Health Sciences, Niigata, Japan;
[3]Department of Pediatric Surgery, Niigata University Graduate School of Medical and Dental Sciences, Niigata, Japan

Abstract. *Background/Aim: Sorafenib is a multikinase inhibitor approved as a first-line therapy for hepatocellular carcinoma. This study examined the sorafenib resistance mechanism. Materials and Methods: Hepatoma HepG2 cells were exposed to sorafenib, and the biological activity of the conditioned media was analyzed using cell proliferation/apoptosis assays, multiplex immunoassays, ELISA, and western blot analyses. The effect of urokinase-type plasminogen activator (uPA) inhibitors or siRNA-mediated gene silencing was examined in culture experiments and a mouse xenograft tumor model. Results: Sorafenib increased uPA secretion, which was abrogated by an Akt inhibitor. The growth-inhibitory effect of sorafenib was significantly enhanced by the uPA inhibitors UK122 and amiloride. Sorafenib-induced apoptosis was increased 2.4-fold in uPA siRNA-transduced cells ($p<0.05$). Combined therapy with sorafenib and amiloride significantly decreased tumor volumes [mean volume: 759 mm^3 (sorafenib) vs. 283 mm^3 (sorafenib plus amiloride), $p<0.05$]. Conclusion: uPA may play a critical role in sorafenib resistance.*

Hepatocellular carcinoma (HCC) is a common malignant tumor in humans that accounts for over 80% of primary liver cancers (1). The early diagnosis of HCC is difficult because it shows no apparent clinical evidence and most advanced HCC cases are less responsive to chemotherapy (2). Many types of molecular targeting drugs (tyrosine kinase inhibitors and immune-control point inhibitors) are now available for treating advanced HCC. However, the sequence or switching time between these agents is unclear. For patients who have not completed the first-line molecular targeted therapy, second-line treatment should be performed taking into account the efficacy and side-effects of the previous treatment (3, 4). To increase systemic treatment options for advanced HCC, an approach for overcoming the resistance to the first-line molecular targeted therapy is essential.

Sorafenib (Nexavar, BAY 43-9006), a multikinase inhibitor that targets Raf, vascular endothelial growth factor receptor (VEGFR), and platelet-derived growth factor receptor (PDGFR) (5), is a first-line molecular targeted agent approved for treating advanced HCC. Sorafenib targets high tyrosine kinase activity in HCC, making its therapeutic effect biologically plausible. However, in clinical settings, sorafenib improves the overall survival of patients by only approximately 3 months, and it rarely leads to tumor disappearance or shrinkage (6, 7). Clinical trials have studied the combination of sorafenib and standard chemotherapies, and assessments of the clinical tolerance and efficacy of combination therapies are still ongoing. For example, several studies have reported that a combination of sorafenib and transarterial chemoembolization (TACE) provides benefits in tumor-time progression (TTP) in HCC patients, whereas others reported less improvement (8, 9). A recent clinical trial of treatment with sorafenib plus a standard systemic chemotherapy regimen (mFOLFOX: 5-fluorouracil, leucovorin, and oxaliplatin) has reported a slightly superior TTP in HCC patients compared with treatment with sorafenib alone; Of note, it also cautioned that patients should be selected carefully in consideration of the hepatotoxicity of the treatment (10).

Experimental studies have suggested that sorafenib resistance is caused by various types of deregulated intracellular mechanisms such as phosphoinositide 3-kinase

Correspondence to: Yasunobu Matsuda, MD, Department of Medical Technology, Niigata University Graduate School of Health Sciences, 2-746 Asahimachi-dori, Chuo-Ku, Niigata 951-8518, Japan. Tel: +81 252270958, Fax: +81 252270749, e-mail: yasunobu@med.niigata-u.ac.jp

Key Words: Sorafenib, drug resistance, urokinase-type plasminogen activator, hepatocellular carcinoma.

(PI3K)/Akt signaling, Janus kinase (JAK)/signal transducer and activator of transcription (STAT) signaling, hypoxia-inducible pathways, and noncoding RNAs (11, 12). Currently, no clinically proven safe agents that directly target these molecules are available. Additional knowledge about the sorafenib resistance mechanism can allow the development of a clinically tolerated combined therapy.

Until recently, only a few studies had reported that sorafenib upregulates the secretion of growth factors or chemokines in hepatoma cells, such as hepatocyte growth factor (HGF), VEGF, and C-C motif chemokine ligand 22 (CCL22) (13-15). These studies strongly suggest that antagonizing soluble factors might be a new potential scheme for enhancing the efficacy of molecular targeted therapies in HCC. Unfortunately, the sorafenib resistance mechanism based on soluble factors remains understudied. Therefore, we decided to determine whether soluble factors could be implicated in sorafenib resistance. We tested our hypothesis by addressing whether the conditioned medium of sorafenib-treated cultured hepatoma cells exerts potential effects on the drug resistance, and we sought to identify candidate molecules that attenuate the antitumor effect of sorafenib. Moreover, to determine the clinical utility of our results, we examined whether chemical or pharmacological inhibitors of these soluble factors enhance the cell-killing effect when combined with sorafenib. The aim of our study was to identify whether soluble factors play a role in sorafenib resistance and to examine its potential as a target of combined therapy in advanced HCC.

Materials and Methods

Reagents. Sorafenib (Toronto Research Chemicals, North York, ON, Canada) was used at a concentration of 5-10 μM in the cytotoxicity experiments; this is equivalent to the plasma drug concentration levels in cancer patients (16, 17). LY294002 (a biochemical inhibitor of PI3K/Akt; Cell Signaling Technology, Beverly, MA, USA), UK122 (a selective urokinase-type plasminogen activator (uPA) inhibitor; Santa Cruz Biotechnology, Santa Cruz, CA, USA), amiloride hydrochloride dehydrate (amiloride, a potassium-sparing diuretic that acts as a selective uPA inhibitor; Santa Cruz Biotechnology), and Z-VAD-FMK (cell permeable pan-caspase specific inhibitor; Enzo Life Sciences, Farmingdale, NY, USA) were used at concentrations of 25, 10, 100, and 20 μM, respectively. All compounds were dissolved in dimethyl sulfoxide (DMSO), and the final DMSO concentration was set to 0.1% in the cell culture.

A polyclonal antibody recognizing uPA was obtained from Proteintech Group (Rosemont, IL, USA), and rabbit monoclonal antibodies against matrix metalloproteinase (MMP)-2, MMP-9, phospho-p44/42 MAPK (ERK1/2) (Thr202/Tyr204), phospho-Akt (Ser473), phospho-p38 MAPK (Thr180/Tyr182), p-SAPK/JNK (Thr183/Tyr185), and cleaved PARP (Asp214) were obtained from Cell Signaling Technology (Beverly, MA, USA). A mouse monoclonal antibody recognizing β-actin was obtained from Sigma-Aldrich Chemical (St Louis, MO, USA).

Cell culture. Human hepatoma HepG2 cells (American Type Culture Collection, Manassas, VA, USA) were maintained in Dulbecco's modified Eagle's medium (DMEM; Sigma-Aldrich) with 10% fetal bovine serum (FBS) at 37˚C in a humidified atmosphere of 5% CO_2.

Collection of conditioned media. To obtain the conditioned media of sorafenib-treated cells, cells (10×10^5 cells/ml) were cultured with or without 7.5 μM sorafenib for 20 h. To minimize the effect of the residual reagent remaining on the cell surface or in the culture media, cells were washed three times with a sufficient amount of phosphate buffered saline (PBS) and maintained for a further 24 h in 10% FBS-supplemented fresh media. The cell culture supernatant was then recovered, centrifuged at 180 g for 3 min, and filtered through a 0.22 μm pore size filter to remove cell debris. The conditioned media of the control cells were termed CONT-CM, and that of sorafenib-treated cells were termed SOR-CM. They were stored at –80˚C and gradually warmed to 37˚C before use. Cells were cultured under CONT-CM or SOR-CM and allowed to react with sorafenib for 24-48 h.

Bio-Plex multiplex immunoassay. HepG2 cells were treated with 7.5 μM sorafenib for 24 h, and supernatants of the culture medium were centrifuged at 180 g for 3 min and filtered through a 0.22-μm pore size filter for removing cell debris. Cytokine concentrations in the samples were measured using Bio-Plex Pro™ Human Cancer Biomarker Panel 1 kit (Bio-Rad Laboratories, Hercules, CA, USA) according to the manufacturer's instructions. This kit contains a mixture of magnetic bead-based assays for analyzing biomarker proteins known to play roles in the angiogenesis, metastasis, and cell proliferation (details are shown in Table I). Experiments were performed in duplicate, and the concentration of each biomarker was calculated using a standard curve provided by the manufacturer.

Proteome profiler antibody array. HepG2 cells were treated with 5 μM sorafenib for 48 h, and the supernatants of the culture medium were centrifuged at 180 g for 3 min, filtered through a 0.22-μm pore size filter, and collected for analyses. The expression profiles of 55 cytokines in the collected samples were examined using Proteome Profiler Human Angiogenesis Array kit (R&D Systems, Minneapolis, MN, USA), a membrane-based sandwich immunoassay, according to the manufacturer's instructions.

Briefly, aliquots of the conditioned media were mixed with a biotinylated antibody cocktail at room temperature for 1 h, and sample/antibody mixtures were incubated with the array membrane spotted in duplicate with each set of capture antibodies at 4˚C for 24 h. Then, the membranes were washed and incubated with streptavidin-conjugated peroxidase for 30 min at room temperature. Proteins bound to the membrane were visualized using a chemiluminescence reagent provided in the kit. The optimal densities of the selected protein were quantified using image analysis software (Image-J, ver. 1.44; NIH, Bethesda, MD, USA), and the data were normalized by reference positive controls spotted on the membrane.

Western blotting. Cell protein lysates were prepared using a modified radioimmunoprecipitation (RIPA) assay buffer (25 mM Tris–HCl pH 7.6, 150 mM NaCl, 1% NP-40, 1% sodium deoxycholate, 0.1% SDS) containing a protease inhibitor cocktail (Roche Diagnostics, Basel, Switzerland). Protein samples (10 μg) were electrophoresed on 10% SDS polyacrylamide gels and transferred onto polyvinylidene difluoride (PVDF) membranes. The

Table I. *Cytokine concentration in the conditioned media.*

Cytokine	CONT (pg/ml)	SOR (pg/ml)	*p*-Value
sEGFR	113.5±9.2	64.8±9.5	0.0005
FGF-basic	33.8±2.7	23.6±4.5	0.0098
Follistatin	46.8±2.5×10^3	17.2±7.0×10^3	0.0002
G-CSF	6.4±0.4	3.8±1.1	0.0043
sHER2/neu	348.1±34.4	253.1±22.9	0.0060
HGF	33.5±3.4	17.7±.3	0.0004
sIL-6Ra	441.0±48.5	262.0±36.0	0.0017
Leptin	59.5±3.9	31.7±7.5	0.0007
Osteopontin	N.D.	N.D.	N.D.
PDGF-AB/BB	6.2±0.6	3.6±0.8	0.0022
PECAM-1	140.2±18.5	53.9±11.3	0.0004
Prolactin	46.3±4.3	25.9±4.5	0.0009
SCF	22.6±1.5	16.6±1.2	0.0012
sTIE-2	316.0±19.6	203.5±54.6	0.0088
sVEGFR-1	135.3±24.1	53.1±11.0	0.0015
sVEGFR-2	53.8±3.1	23.6±4.5	<0.0001

CONT: Conditioned media of the control cells; SOR: conditioned media of sorafenib-treated cells; sEGFR: soluble epidermal growth factor receptor; FGF-basic: fibroblast growth factors; G-CSF: granulocyte colony stimulating factor; sHER2/neu: soluble epidermal growth factor receptor type2/neu; HGF: hepatocyte growth factor; sIL-6Ra: soluble interleukin-6 receptor a; PDGF-AB/BB: platelet derived growth factor-AB/BB; PECAM-1: platelet endothelial cell adhesion molecule-1; SCF: stem cell factor; sTIE-2: soluble TIE-2 (angiopoietin receptor-2); sVEGFR-1: soluble vascular endothelial growth factor-1; sVEGFR-2: soluble vascular endothelial growth factor-2; N.D.: not detected.

membranes were reacted with appropriate primary antibodies and horseradish peroxidase-conjugated secondary antibodies. Protein bands were visualized using an Enhanced Chemiluminescence (ECL) Kit (GE Healthcare, Piscataway, NJ, USA). The band intensities normalized against the β-actin bands were quantified using image analysis software (Image-J, ver. 1.44).

Cell proliferation assay. Cells (0.3×10^5 cells/ml) were plated and cultured on 96-well plates with CONT-CM, SOR-CM or normal DMEM for 24 h and exposed to sorafenib with or without chemical inhibitors for 24 h. Cell proliferation rates were analyzed using a water-soluble tetrazolium (WST) Cell Counting Kit-8 (Dojindo Laboratories, Kumamoto, Japan). The absorbance was analyzed at 450 nm using a Multiscan FC microtiter-plate reader (Thermo Fisher Scientific, Waltham, MA, USA). Each experiment was independently performed in triplicate.

Cell apoptosis assay. Cells (1×10^5 cells/ml) were plated on glass coverslips and treated with sorafenib with or without chemical inhibitors for 24 or 48 h. Annexin V-positive apoptotic cells and annexin V/propidium iodide (PI)-double positive late apoptotic/necrotic cells were stained by using an Annexin V FITC Kit (Invitrogen, Karlsruhe, Germany). The percentages of apoptotic or necrotic cells were evaluated by counting 200 cells in a microscopic high-power field (HPF) with a fluorescence microscope (BZ-9000; Keyence, Osaka, Japan). Each experiment was independently performed in triplicate.

Enzyme-linked immunosorbent assay and uPA activity assay. To determine the levels of uPA secretion, the cell culture supernatant was collected from cells (5×10^5 cells/ml) treated with sorafenib for 48 h. To examine whether sorafenib affected uPA secretion through Akt signaling, LY294002 or Z-VAD-FMK was added 1 h before sorafenib treatment. The uPA levels in the media were evaluated using Quantikine ELISA kits (R&D Systems) according to the manufacturer's instructions.

The uPA activity in the culture media was measured using a colorimetric uPA activity assay kit (Urokinase-type Plasminogen Activator Human Chromogenic Activity Assay Kit; Abcam, Cambridge, UK). Cells (10×10^5 cells/ml) were treated with 5-7.5 μM sorafenib for 24 h. Cell culture supernatants were incubated with the plasmin and chromogenic substrate, provided in the kit, at 37˚C for 2 h. The absorbance at 405 nm was measured in an automated spectrophotometric plate reader (Multiscan FC; Thermo Fisher Scientific, Waltham, MA, USA). The uPA activity was calculated in units of IU/ml using a standard curve prepared in each experiment, as recommended by the manufacturer. All ELISA and uPA activity assay experiments were independently performed in triplicate.

siRNA transfection. We obtained several siRNAs directed against the human uPA gene (Hs_PLAU_2, 3, 6, and 7 Flexitube siRNAs; Qiagen, Hilden, Germany) and found that Hs_PLAU_7 Flexitube siRNA (target sequence GAGCTGGTGTCTGATTGTTAA; Catalogue No. SI02662674) was the most efficient for reducing the uPA mRNA and protein expression in HepG2 cells (data not shown). Therefore, we used this siRNA for the specific inhibition of uPA gene expression as well as Negative Control siRNA (Catalogue No. 1022076; Qiagen). Cells (1×10^5 cells/ml) were treated with siRNAs using HiPerfect Transfection Reagent (Qiagen) according to the manufacturer's guidelines. After 48 h of transfection, the cells were treated with sorafenib for 24 h and used for further analysis.

Cell motility assay. The low-dose sorafenib-induced invasive abilities of cells transfected with siRNA were analyzed using a cell migration assay and a wound healing assay. The cell migration assay was performed using 8 μm pore-24 well Transwell Boyden chamber plates (BD Biosciences, San Jose, CA, USA). Cells were treated with 0.5 μM sorafenib for 24 h, and 0.3×10^5 trypsinized cells were seeded onto the upper compartment of the plates. To induce a chemotactic gradient of FBS, the upper compartment was filled with 1% FBS-supplemented DMEM and the lower compartment was filled with the same media containing 10% FBS. After 24 h, the cells that migrated to the lower surface of the membrane were fixed by methanol and visualized by Giemsa staining. Migrated cells were counted in three random microscopic fields. The wound healing assay was performed by making a linear wound on a confluent cell monolayer using a 2-mm-wide tip. Cells treated with low-dose sorafenib (0.5 μM) for 24 h were allowed to migrate, and the wound closure ratio was observed with a phase-contrast microscope. Each experiment was independently performed in triplicate.

Animal model. Male 6-week-old Balb/c nu/nu mice were obtained from CLEA (Tokyo, Japan) and housed in pathogen-free controlled conditions. All procedures were performed carefully to minimize any suffering in mice according to the National Institutes of Health guidelines for the care and use of laboratory animals. Animal experiments were approved by the Institutional Animal Care and

Use Committee at Niigata University Graduate School of Medical and Dental Sciences (Niigata, Japan) under Assurance Number H26-139. To develop a xenograft mouse model, mice were inoculated with HepG2 cells (1.0×10^6 cells mixed with BD Matrigel Matrix; BD Biosciences) at the right flank via subcutaneous injection. The tumor volume and body weight were recorded every 3 days. When the tumor volume reached 300 mm^3, mice were randomly categorized into four groups (n=7 in each): 1) control (vehicle), 2) sorafenib (10 mg/kg/day), 3) amiloride (5 mg/kg/day), and 4) sorafenib (10 mg/kg/day) plus amiloride (5 mg/kg/day). All reagents were administered daily by gavage. The drug preparation and dosage have been described in previous studies. Sorafenib was dissolved in 12.5% Cremophor EL/12.5% ethanol in sterile water, and amiloride was dissolved in sterile distilled water with warming. We preliminarily observed that tumors grew rapidly, and some mice in the control group developed an ulceration at the tumor sites 15 days after starting drug administration (not shown). Therefore, the mice were administered the reagents for a total of 12 days and euthanized 24 h after the last administration. After the tumors were excised from the body, tumor volumes were measured with calipers and calculated using the following modified ellipsoid formula: volume (mm^3)=$width^2$ × length ×0.5. The excised tumors were immediately stored in neutral phosphate-buffered 10% formalin and processed for paraffin embedding. Tumor tissue sections were deparaffinized and processed for hematoxylin and eosin (H&E) staining and immunostaining.

Immunohistochemistry. For analyzing the effect of the drug on tumor cell proliferation, tumor tissue sections were rehydrated and subjected to antigen retrieval by microwave in citrate buffer (pH 6.0). Tissue sections were reacted with anti-Ki-67 (D2H10) rabbit monoclonal antibody (1:100) (IHC-specific; Cell Signaling Technology) or anti-PCNA rabbit polyclonal antibody (1:100) (Santa Cruz Biotechnology) at 4˚C overnight. Immunostaining was visualized using the Elite ABC kit (Vector Laboratories, Burlingame, CA, USA) with 3,3'-diaminobenzidine, and counterstaining was performed using hematoxylin. The labeling indices (LI) for PCNA and Ki-67 were calculated as the number of positive nuclei in 100 tumor cells in three randomly selected fields using a Primo Star light microscope (Carl Zeiss, Oberkochen, Germany).

Statistical analysis. The significance of differences among groups was evaluated using Student's *t*-test for two groups. The data are presented as the mean±standard deviation (SD) of individual experiments. Bar graphs indicate the mean data, and error bars indicate SDs. *p*-Values of 0.05 were considered statistically significant.

Results

Culture media of sorafenib-treated cells induce drug resistance. We first determined whether sorafenib treatment triggers the secretion of factors inducing drug resistance in hepatoma cells. For this purpose, HepG2 cells were incubated with conditioned media derived from cells treated with and without sorafenib (SOR-CM and CONT-CM, respectively). We found that the antitumor effect of sorafenib was attenuated in cells incubated with SOR-CM. The WST assay showed that the inhibitory effect of 7.5 μM sorafenib treatment for 24 h on cell growth was suppressed in cells incubated with SOR-CM compared with that in cells incubated with CONT-CM (absorbance value: 0.83±0.05 (cells incubated with CONT-CM) *vs*. 1.35±0.07 (cells incubated with SOR-CM), $p<0.01$; Figure 1A). An annexin V assay performed after 10 μM sorafenib treatment for 48 h demonstrated that the percentage of annexin V-positive apoptotic cells was 34±5% in cells incubated with CONT-CM *versus* 7±3% in those incubated with SOR-CM ($p<0.01$; Figure 1B). The ratio of PI-positive necrotic cells was 25±5% in cells incubated with CONT-CM *versus* 4±3% in cells incubated with SOR-CM ($p<0.01$).

uPA is increased in sorafenib-treated cell culture media. Next, we evaluated the cytokine profiles secreted in response to sorafenib treatment using a 16-plex magnetic-bead-based immunologic assay (Bio-Plex™ Human Cancer Biomarker Kit) (Table I) and a 55-plex sandwich membrane immunologic assay (Proteome Profiler Human Angiogenesis Array Kit) (Figure 2).The concentrations of most cytokines decreased or remained unchanged following sorafenib treatment, whereas dipeptidyl peptidase IV (DPPIV), insulin-like growth factor binding protein-1 (IGFBP-1), and uPA concentrations were statistically significantly increased in SOR-CM ($p<0.01$). Among them, uPA was found to be most remarkably increased (DPPIV; 1.3-fold, IGFBP-1; 1.5-fold, uPA; 1.9-fold) (Figure 2). The ELISA analysis revealed that sorafenib treatment induces uPA secretion in the culture media (92.3±3.5 pg/ml (control) *vs*. 272.3±17.7 pg/ml (sorafenib), $p<0.01$; Figure 3A). The uPA activity was measured through a colorimetric assay. Figure 3B shows that uPA activity levels in the conditioned medium of sorafenib-treated cells were significantly increased (control; $1.3\pm1.2\times10^{-3}$ IU/ml *vs*. sorafenib 5 μM; $57.8\pm10.6\times10^{-3}$ IU/ml *vs*. sorafenib 7.5 μM; $138.6\pm9.6\times10^{-3}$ IU/ml, $p<0.01$ and $p<0.01$ *vs*. control, respectively), suggesting that uPA released following treatment with sorafenib is bioactive. Western blot analyses of cell lysates showed a 2.3- to 3.4-fold increase in uPA concentrations in sorafenib-treated cells compared to controls (less than $p<0.05$; Figure 3C). MMP-2 and MMP-9 were also analyzed using western blot analysis, and no significant changes were observed between controls and sorafenib-treated cells (MMP-2 and MMP-9; 1.3-1.6 -fold and 0.5-0.7 fold, respectively, $p>0.05$ and $p>0.05$ *vs*. control, respectively; Figure 3C).

Akt/uPA signaling mediates drug resistance. We evaluated whether stress-activated protein kinases are involved in sorafenib-mediated uPA secretion. The results of western blot analyses of cellular lysates showed that sorafenib treatment decreased the phosphorylation levels of ERK1/2, p38MAPK, and SAPK/JNK whereas it significantly increased the levels of phosphorylated Akt [30.6-fold (mean) of control, $p<0.01$; Figure 4A]. The uPA concentration in sorafenib-treated cell

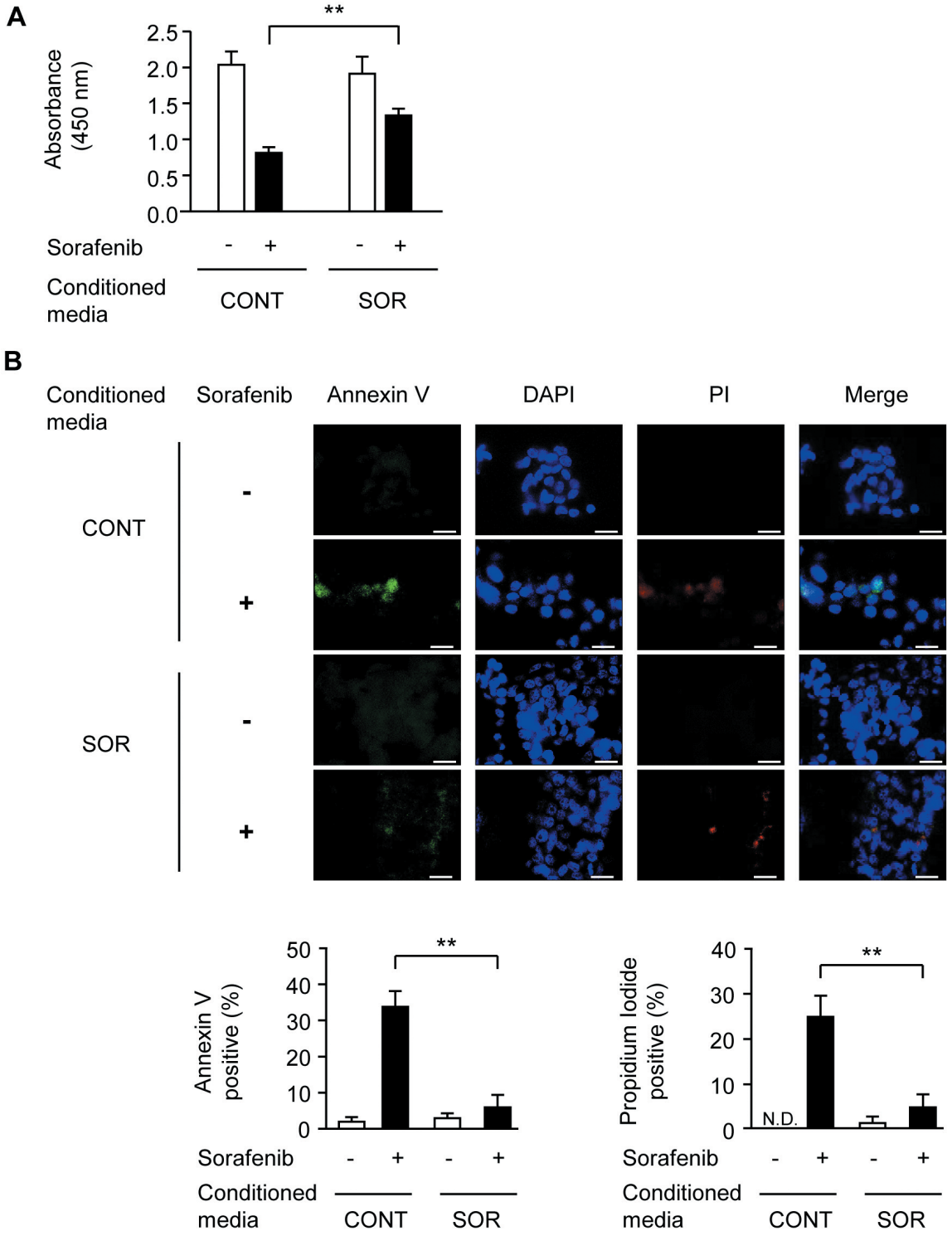

Figure 1. *Conditioned media of sorafenib-treated cells induce drug resistance. (A) WST cell proliferation assay of Hep2 cells. Cells were cultured in conditioned media of control cells (CONT-CM) or cells previously treated with sorafenib (SOR-CM), and subsequently were treated with 7.5 μM sorafenib for 24 h. Columns represent mean absorbance (optical densities) for cell growth at 450 nm. (B) Representative images of apoptotic or late-apoptotic/necrotic cells. Cells were cultured under CONT-CM or SOR-CM and then treated with 10 μM sorafenib for 48 h. White and black columns indicate control and sorafenib-treated cells, respectively. Data are presented as the mean±standard deviation (SD) of independent experiments in triplicate (**p<0.01). CONT: Conditioned media of control cells (CONT-CM); SOR: conditioned media of cells treated with 5 μM sorafenib for 24 h (SOR-CM); DAPI: counter staining with 4',6-diamidino-2-phenylindole; PI: propidium iodide; N.D.: not detected.*

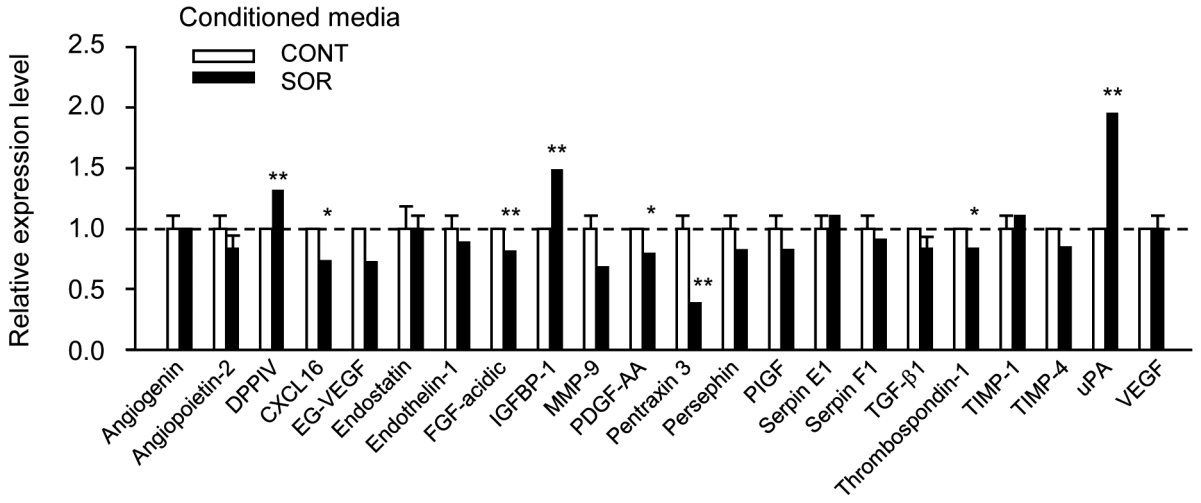

Figure 2. *uPA is increased in the sorafenib-treated cell culture. Levels of 55 cancer-related proteins were analyzed in the conditioned media of HepG2 cells using the Proteome Profiler Human Angiogenesis Array kit. Twenty-two proteins were detected at relatively high levels, and columns represent mean pixel densities of the protein spots. White and black columns indicate control and sorafenib-treated cell culture media, respectively. Data are presented as the mean±SD of two independent experiments (*p<0.05; **p<0.01 vs. control).*

culture media was suppressed by LY294002 but not by Z-VAD-FMK [301.3±9.3 (sorafenib alone) *vs.* 333.0±2.4 (sorafenib plus Z-VAD-FMK) *vs.* 53.0±2.4 pg/ml (sorafenib plus LY294002), $p>0.05$ and $p<0.01$ *vs.* sorafenib alone, respectively; Figure 4B], indicating that uPA secretion is mediated through Akt but not by cell damage.

We then examined whether Akt and uPA play a role in drug resistance induced by SOR-CM. As shown in Figure 4C, WST assays showed that cells pretreated with uPA inhibitors and then incubated with SOR-CM displayed significantly reduced proliferation compared with the use of sorafenib alone [absorbance value: 1.45±0.26 (sorafenib alone) *vs.* 0.78±0.12 (sorafenib plus UK122) *vs.* 0.52±0.16 (sorafenib plus amiloride), $p<0.05$ and $p<0.01$ *vs.* sorafenib alone, respectively]; these were comparable to the levels in cells treated with sorafenib and LY294002 (absorbance value: 0.48±0.05, $p<0.05$ *vs.* sorafenib alone). Together, these results suggest that both Akt and uPA are essential for SOR-CM-mediated drug resistance.

Combination treatment with sorafenib and uPA inhibitors overcomes drug resistance. The results of WST assays confirmed a significant improvement in the antitumor effect of sorafenib in combination with uPA inhibitors. WST assays showed that treatment with UK122 or amiloride alone resulted in a small but not significant reduction in cell proliferation (UK122 and amiloride; $p>0.05$ and $p>0.05$ *vs.* control, respectively) (Figure 5A). Upon treatment with the combination of sorafenib and uPA inhibitors, cell proliferation levels were significantly reduced in comparison with the use of sorafenib alone (absorbance value: 0.61±0.02 (5 μM sorafenib alone) *vs.* 0.41±0.09 (sorafenib plus UK122) *vs.* 0.30±0.04 (sorafenib plus amiloride), $p<0.05$ and $p<0.01$ *vs.* sorafenib alone, respectively; absorbance value: 0.50±0.02 (7.5 μM sorafenib alone) *vs.* 0.24±0.03 (sorafenib plus UK122) *vs.* 0.21±0.04 (sorafenib plus amiloride), $p<0.01$ and $p<0.01$ *vs.* sorafenib alone, respectively; Figure 5A).

An annexin V assay showed that treatment with the combination of sorafenib and uPA inhibitors significantly increased the number of apoptotic and necrotic cells. Treatment with UK122 or amiloride alone led to a non-significant increase in the rates of annexin V-positive apoptotic cells [2±1% (control) *vs.* 2±2% (UK122) *vs.* 12±4% (amiloride), $p>0.05$ and $p>0.05$ *vs.* control, respectively] (Figure 5B). By contrast, the percentages of annexin V-positive cells were 29±4%, 41±4%, and 59±6% of the cells treated with sorafenib alone, sorafenib plus UK122, and sorafenib plus amiloride, respectively ($p<0.05$ and $p<0.01$ *vs.* sorafenib alone, respectively; Figure 5B). The ratios of PI-positive necrotic cells were 18±3%, 27±2%, and 31±4% in cells treated with sorafenib alone, sorafenib plus UK122, and sorafenib plus amiloride, respectively ($p<0.05$ and $p<0.05$ *vs.* sorafenib alone, respectively; Figure 5B).

uPA knockdown alleviates sorafenib resistance in hepatoma cells. To substantiate the possible role of uPA in sorafenib resistance, siRNA-mediated knockdown of the uPA gene was performed in HepG2 cells. Western blot analyses showed that uPA siRNA interference led to a significant decrease in uPA protein expression (0.3-fold; $p<0.01$), and the cleaved

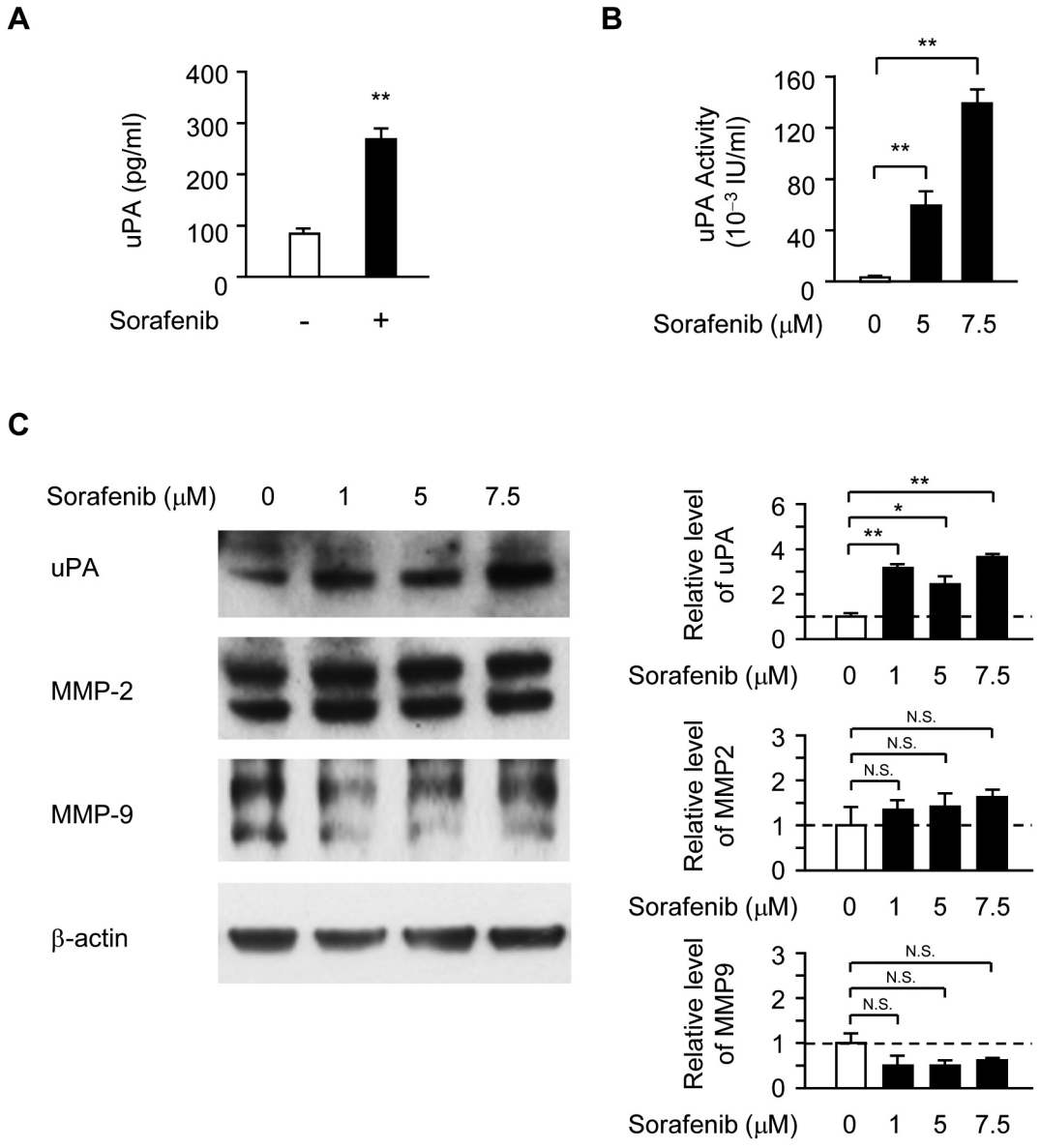

Figure 3. *Sorafenib induces the release of bioactive uPA. (A) uPA ELISA analysis of culture media. Cells were treated with 5 μM sorafenib for 48 h, and the uPA concentration in the conditioned medium was analyzed by ELISA. (B) uPA activity in culture media. Cells were treated with different sorafenib concentrations (5-7.5 μM) for 24 h, and uPA activity in conditioned media was measured using a colorimetric kit. (C) Western blot analyses of uPA, MMP-2, and MMP-9 expression. Cells were treated with different concentrations of sorafenib (1-7.5 μM) for 24 h, and cell lysates were used for analyses. Columns represent normalized band intensities relative to β-actin bands based on fold changes compared to controls. White and black columns indicate control and sorafenib-treated cells, respectively. Data are presented as the mean±SD of independent experiments in triplicate (N.S.: not significant, *p<0.05, **p<0.01 vs. control).*

PARP levels after sorafenib treatment increased to 1.8-fold in uPA-siRNA-transduced cells ($p<0.05$ for mock *vs*. uPA siRNA; Figure 6A). WST assays showed that the inhibitory effect of sorafenib on cell proliferation was significantly enhanced in uPA siRNA-transduced cells compared with mock siRNA-transduced cells (absorbance value: 0.63±0.02 (sorafenib-treated mock) *vs*. 0.23±0.03 (uPA siRNA-treated cells), $p<0.01$; Figure 6B). Following sorafenib treatment, the percentages of annexin V-positive and PI-positive cells were significantly increased to 2.4-fold and 5.3-fold, respectively, in uPA siRNA-transfected cells (sorafenib-treated mock *vs*. uPA siRNA; annexin V-positive: 9±3% *vs*.

22±4 %, PI-positive: 3±2% *vs.* 16±2%, $p<0.05$ and $p<0.05$, respectively; Figure 6C).

uPA knockdown reduces cell migration induced by low-dose sorafenib. We also evaluated whether uPA is involved in low-dose sorafenib-induced cell migration. A cell migration assay showed that following low-dose (0.5 μM; nontoxic concentration) sorafenib treatment, cell migration was increased in mock siRNA-transduced cells (12±4 cells/HPF (control) *vs.* 40±5 cells/HPF (sorafenib), $p<0.01$). This effect was substantially suppressed in uPA siRNA-transfected cells (26±2 cells/HPF, $p<0.05$ *vs.* sorafenib-treated mock siRNA-transfected cells; Figure 7A). Wound healing assays showed that wound closure by migrating cells was significantly promoted by treatment with low-dose sorafenib in mock siRNA-transfected cells, whereas it was repressed in uPA siRNA-transfect cells [10±2% (control mock siRNA) *vs.* 35±6% (sorafenib-treated mock siRNA) *vs.* 13±5% (sorafenib-treated uPA siRNA), $p<0.05$ for sorafenib-treated cells with mock *vs.* uPA siRNA; Figure 7B).

Therapeutic effect of the treatment with the combination of sorafenib and amiloride in vivo. To examine the *in vivo* effect of the combination treatment with sorafenib and uPA inhibitors, sorafenib and amiloride were administered to the HCC orthotopic model of HepG2 cells. During the experiment, treatment was well tolerated with no weight loss and no critical physiological features (not shown). After administration, all tumors in the control group developed rapidly, ranging in size from 700 to 1,440 mm^3 (1,080±283 mm^3; Figure 8A). In the sorafenib-treated group, the tumor volume was numerically but not statistically significantly decreased (759±338 mm^3, $p>0.05$ *vs.* control). In the amiloride-alone treated group, tumors were variable in size and showed no apparent change from the control group (1,331±865 mm^3, $p>0.05$ *vs.* control). The combination treatment with sorafenib and amiloride resulted in significant tumor volume regression in all mice, ranging from 144 to 550 mm^3 (283±136 mm^3, $p<0.01$ and $p<0.05$ *vs.* control and sorafenib alone, respectively). These findings indicate that amiloride alone is incapable of regressing tumor volume *in vivo*, but it has a marked antitumor effect when combined with sorafenib.

HE staining of the tumor section showed that all tumors in the control group comprised dense and viable cancer cells. In groups treated with sorafenib alone and amiloride alone, microscopic foci of hemorrhage were observed in the tumors. By contrast, in the group treated with a combination of sorafenib and amiloride, the tumor cell architecture was destroyed and macroscopic necrotic areas filled with hemorrhage were distributed in all tumor tissue sections examined (Figure 8B). Immunostaining results showed that treatment with sorafenib alone decreased the percentages of both PCNA and Ki-67-positive cells slightly but not statistically significantly compared to controls [PCNA: 70±8% (control) *vs.* 61±9% (sorafenib alone); Ki-67: 36±6% (control) *vs.* 35±6% (sorafenib alone); $p>0.05$ and $p>0.05$ *vs.* control, respectively], and treatment with amiloride alone did not cause any significant changes in these markers (PCNA: 73±10%, Ki-67: 40±3%; $p>0.05$ and $p>0.05$ *vs.* control, respectively). In the group with the combination of sorafenib and amiloride, there was a significant reduction in the percentage of PCNA and Ki-67 positive cells (PCNA: 29±10%, Ki-67: 21±3%, $p<0.01$ and $p<0.01$ *vs.* control, respectively; Figure 8B). Together, these findings suggest that tumor cell growth is only inhibited when sorafenib is administered in combination with amiloride.

Discussion

Here, we showed for the first time that sorafenib induces uPA secretion, leading to acquired drug resistance in hepatoma cells. To investigate the mechanism of soluble factor-mediated sorafenib resistance, human hepatoma cells were incubated with SOR-CM and subsequently exposed to sorafenib. The results showed that cell proliferation rates were 1.6 times higher and that the ratio of apoptotic cells was reduced to 0.2 times relative to cells incubated with CONT-CM, supporting the idea that sorafenib stimulates cancer cells to release bioactive substances. The contribution of senescence-associated secretory phenotype (SASP) factors (18) is unlikely as we observed no increase in the expression of SASP markers such as interleukin (IL)-1β, IL-6, p16, and high-mobility group protein B1 (HMGB1) in cells subjected to sorafenib (data not presented).

Given the limited understanding of sorafenib resistance due to soluble factors (13-15), we sought to identify molecular profiles in cell culture media. A total of 71 cytokine expression patterns were analyzed, and the obtained data indicated a remarkable increase in uPA protein concentration and activity in sorafenib-treated cell culture media. In our study, many other cytokines, including HGF and VEGF, that have been reported to be increased with sorafenib treatment (13, 14) were decreased or unaffected. We used HepG2 cells as a common model for *in vitro* studies (19) and used sorafenib at a concentration equivalent to the plasma concentrations of patients receiving sorafenib (16, 17). Further studies are necessary to understand the reason for the different data in different studies.

The mechanism of increasing uPA production is intriguing. MMP-2 and MMP-9 expression levels were not closely correlated with those of uPA in sorafenib-treated cells, implying that the erythroblast transformation-specific (ETS) transcription factor, a common transcription factor of uPA and MMPs (20), is unlikely to be involved. As reported in previous studies including our own (21, 22), sorafenib significantly increased Akt phosphorylation. The uPA

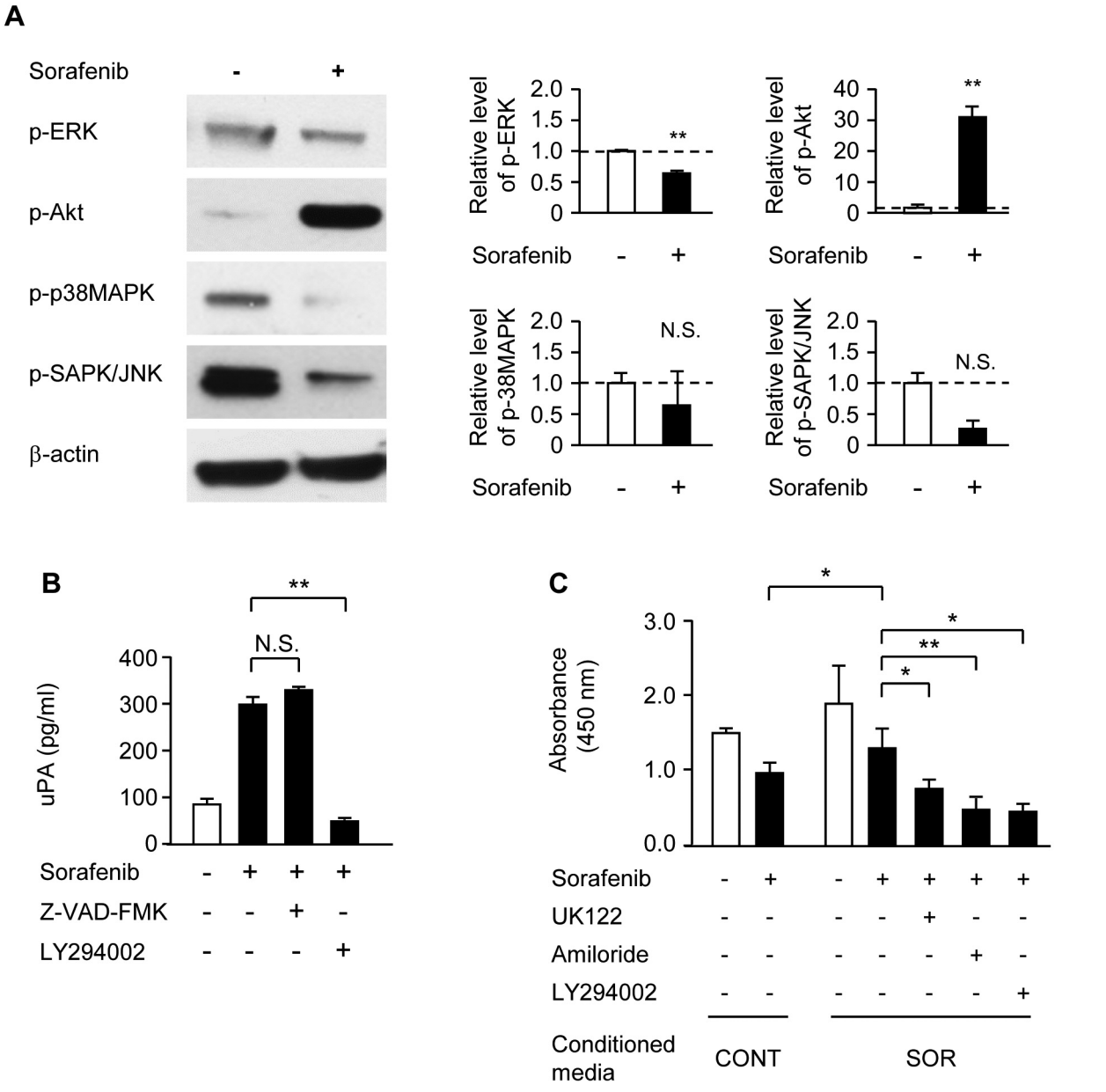

Figure 4. *uPA secretion is mediated through Akt signaling. (A) Western blot analysis of phosphorylated stress-activated protein kinases in sorafenib-treated cells (7.5 μM for 12 h). Columns represent band intensities normalized against β-actin bands as fold changes relative to controls. (B) uPA ELISA analysis of culture media. Cells were treated with 5 μM sorafenib for 48 h with or without pretreatment with Z-VAD-FMK or LY294002 for 1 h. (C) WST cell proliferation assay. Cells were incubated with CONT-CM (CONT) or SOR-CM (SOR) and then treated with 5 μM sorafenib for 24 h with or without pretreatment with UK122, amiloride, or LY294002 for 1 h. White and black columns indicate control and sorafenib-treated cells, respectively. Data are presented as the mean±SD of independent experiments in triplicate [N.S., not significant, (A) **p<0.01 vs. control, (B and C) *p<0.05 and **p<0.01 vs. cells treated with sorafenib alone, respectively].*

concentrations in sorafenib-treated cell culture media were reduced to the control levels using the Akt inhibitor LY294002. Most importantly, treatment with the combination of sorafenib and uPA inhibitors eliminated drug resistance almost equivalently to the cells receiving the combination treatment of sorafenib and LY294002. These data suggest that Akt activation induces uPA production, leading to sorafenib resistance.

uPA is a serine protease that catalyzes the cleavage of plasminogen to plasmin, and it is implicated in tumor

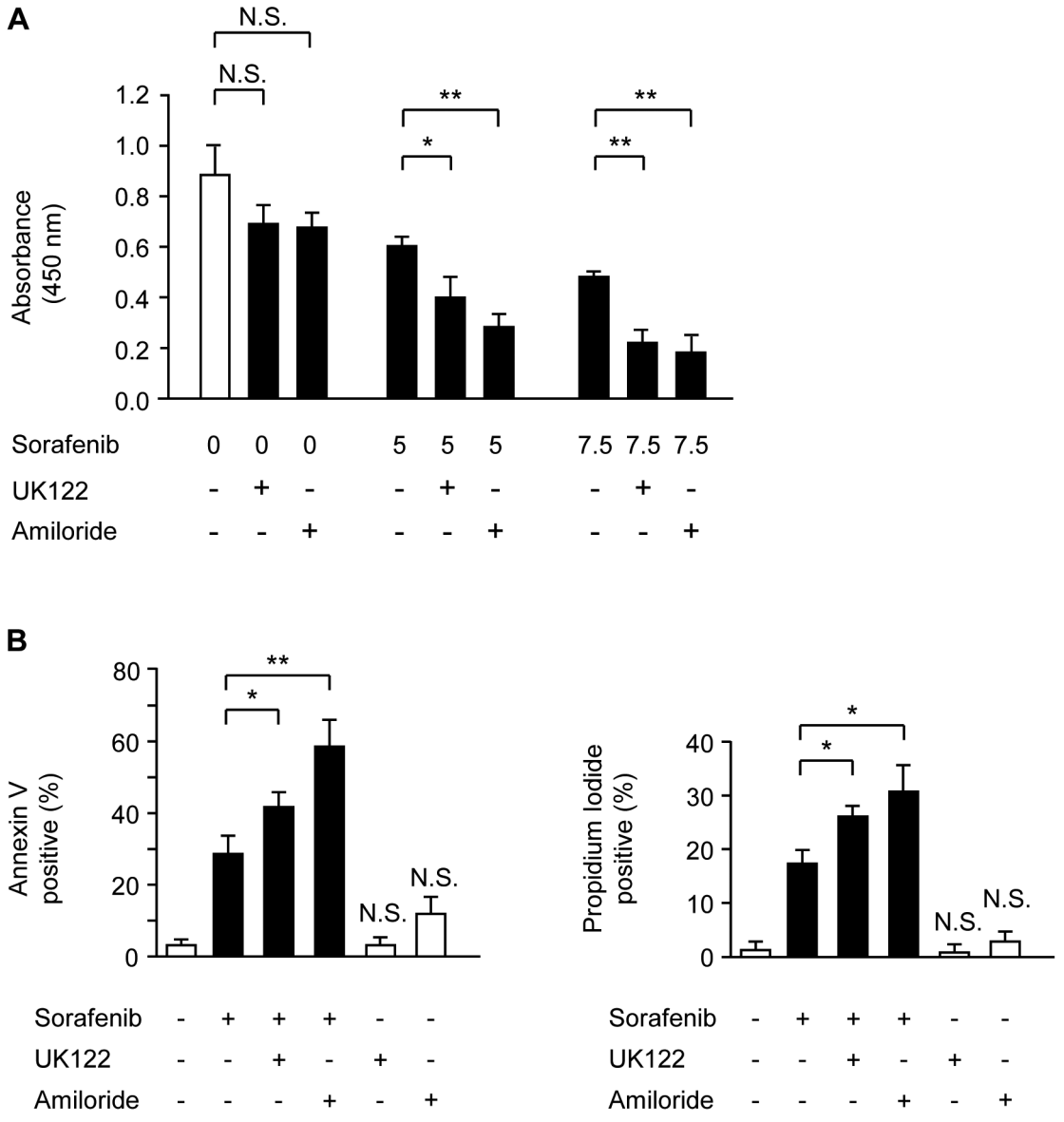

Figure 5. *Combination treatment with sorafenib and uPA inhibitors relieves drug resistance. (A) WST cell proliferation assay. Cells were subjected to different concentrations of sorafenib (5 or 7.5 μM) with or without UK122 or amiloride for 24 h. (B) Percentages of apoptotic and late-apoptotic/necrotic cells as evaluated by annexin V and propidium iodide labeling. Cells were treated with 10 μM sorafenib with or without UK122 or amiloride for 48 h. White and black columns indicate cells without and with sorafenib treatment, respectively. Data are presented as the mean±SD of independent experiments in triplicate (N.S.: not significant, *p<0.05, **p<0.01).*

progression, metastases, and chemoresistance in a wide range of cancers (23, 24). To date, only a few studies have investigated the role of uPA on chemoresistance in HCC. A previous study has reported the therapeutic effects of combination treatment with microRNAs (miRNA)-193a and sorafenib in cancer cells (25). Because miRNA-193a is a suppressive miRNA targeting uPA and several oncogenes (26), it is reasonable to evaluate the direct role of uPA on sorafenib resistance in HCC. In this study, we found that the cell-killing effects of uPA inhibitors were not significant; however, they were significantly increased upon combination with sorafenib. Sorafenib treatment on uPA siRNA-transfected cells led to a substantial increase in cleaved PARP and the number of dead cells. Together, it is highly likely that uPA plays a critical role in sorafenib resistance in HCC. We also observed that sorafenib-mediated cell migration was suppressed in uPA

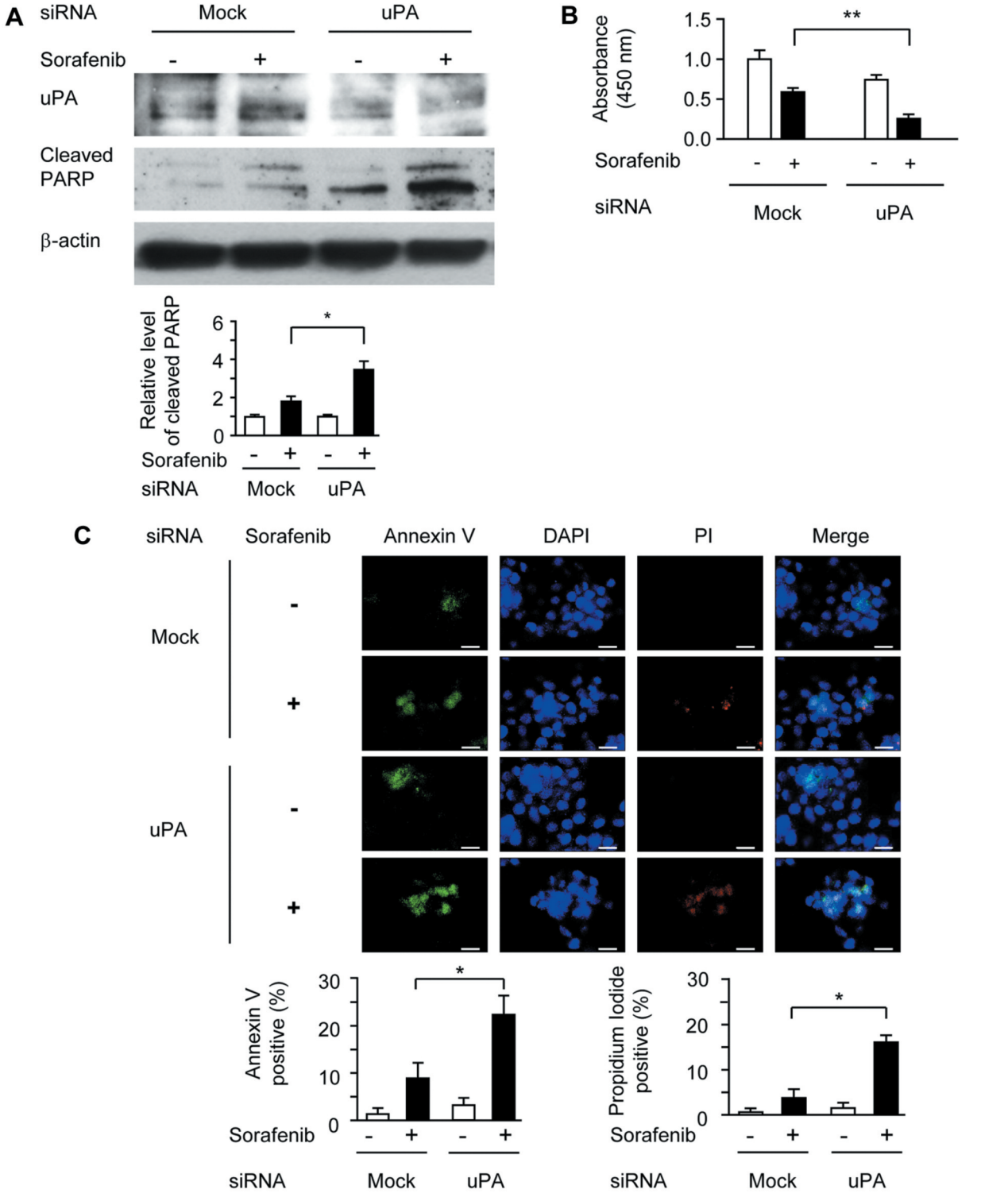

Figure 6. *Knockdown of the uPA mRNA increases the cell-killing effect of sorafenib. (A) Western blot analysis of the cells transfected with a control mock siRNA or uPA-targeting siRNA and exposed to 7.5 μM sorafenib for 20 h. The band intensities of uPA and cleaved PARP normalized by β-actin were expressed as the fold changes relative to the control. (B) Effect of uPA mRNA knockdown was analyzed using the WST cell proliferation assay. Cells were treated with 5 μM sorafenib for 24 h. (C) Antitumor effect of the knockdown of the uPA mRNA was assessed by labeling with annexin V and propidium iodide. White and black columns indicate control and sorafenib-treated cells, respectively. Data are presented as the mean±SD of triplicate experiments (*p<0.05, **p<0.01). DAPI: 4',6-diamidino-2-phenylindole; PI: propidium iodide.*

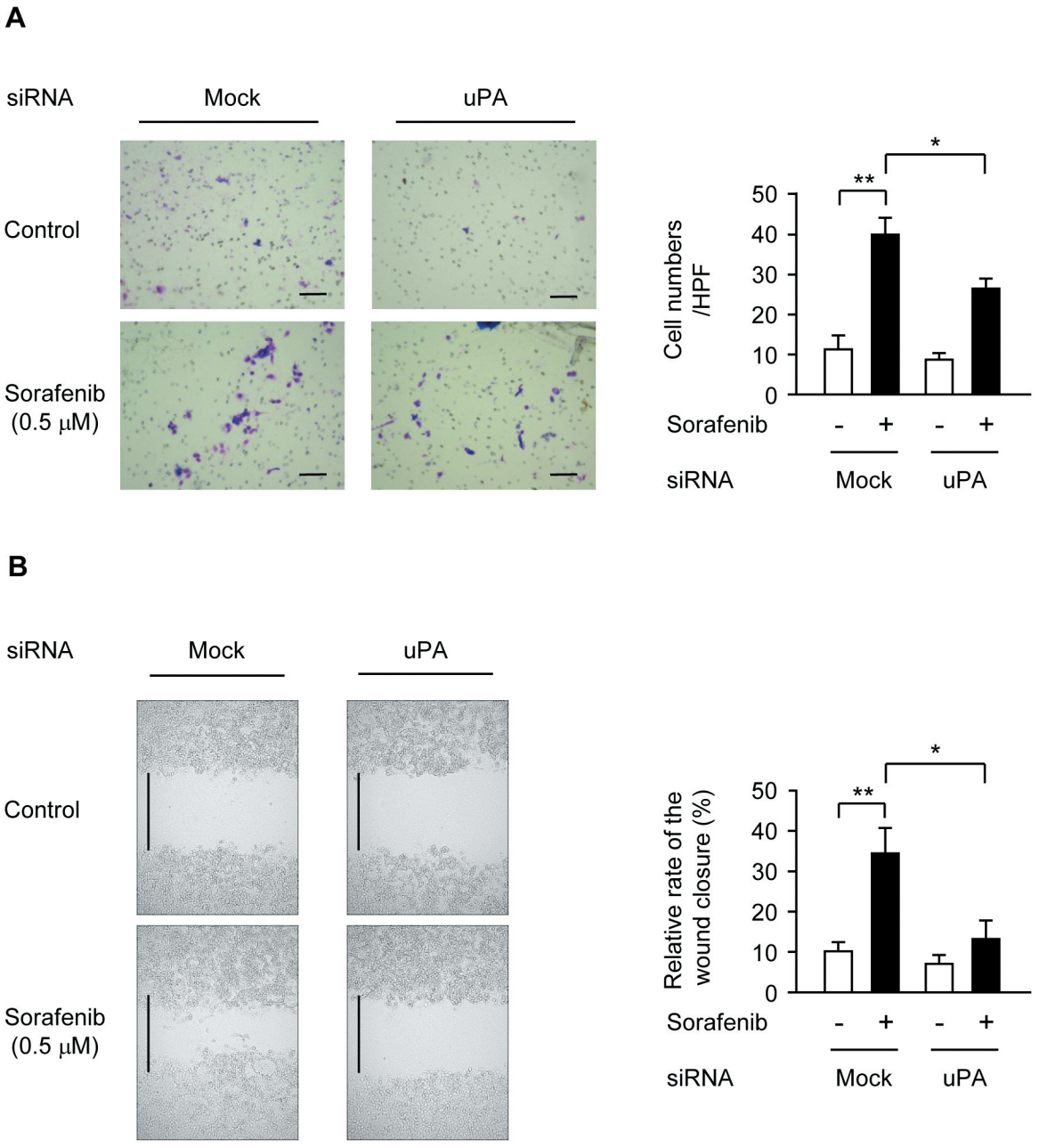

Figure 7. *Blockage of uPA gene expression suppresses low-dose sorafenib-induced cell migration. (A) Representative photographs from the cell migration assay (bar, 100 μm). (B) Representative photographs from wound healing assay (bar, 500 μm). White and black columns indicate control and sorafenib-treated cells, respectively. Data are presented as the mean±SD of triplicate experiments (*p<0.05, **p<0.01).*

siRNA transfected cells. Sorafenib induces cellular migration at lower doses (<1 μM) (27), and the Akt/actin depolymerization factor (cofilin) pathway was found to be critical for cytoskeletal reorganization (28). As the uPA system is involved in the Rho-related GTP-binding protein RhoB-mediated cofilin regulation (29), our data may suggest that Akt/uPA/cofilin signaling may be a potential target for managing sorafenib-induced cancer migration.

To evaluate the clinical importance of our data, we examined the synergistic effects of sorafenib and amiloride in a mouse xenograft tumor model. Amiloride is a moderate inhibitor of sodium hydrogen exchanger isoform 1 (NHE1)

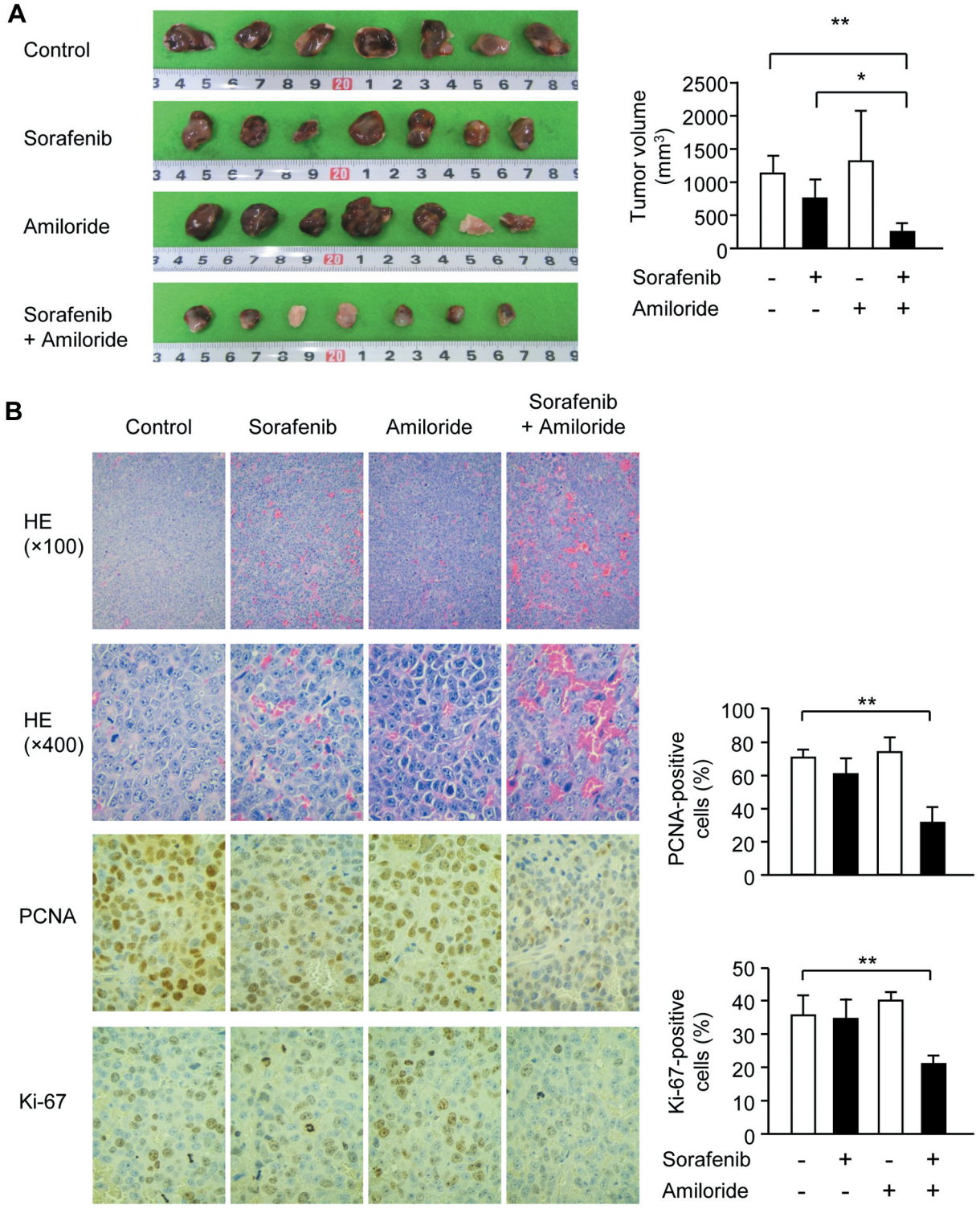

Figure 8. *Combined treatment with sorafenib and amiloride greatly suppresses tumor growth in vivo. (A) Excised tumors in orthotopic mouse model. The scale bars within the images are 0.1 cm. White and black columns indicate the mean tumor volumes of non-sorafenib and sorafenib groups, respectively, and error bars indicate ±SD. (B) Histology of HCC in mouse models. Upper and second panels: low-power field (×100) and high-power field (×400), respectively, of hematoxylin and eosin (HE) staining of tumors in each group. Third and last panel: representative immunostaining images for PCNA and Ki-67, respectively (×400 magnification). White and black columns indicate non-sorafenib and sorafenib-treated groups, respectively. Data are presented as the mean±SD of independent experiments in triplicate (*p<0.05, **p<0.01).*

and has been used as an oral potassium-sparing diuretic. This agent is also known to competitively inhibit the catalytic activity of uPA at low doses without affecting those of tissue-type plasminogen activator, plasmin, plasma kallikrein, or thrombin (30). Our data showed that treatment with the combination of sorafenib and amiloride resulted in a significant regression of tumor growth. Massive necrotic areas with hemorrhage were evident in the tumors of mice receiving the combination treatment; thus, western blot analysis using tissue homogenates was difficult to perform. In line with this observation, immunostaining for cell proliferation markers showed that these tumors were characterized by significantly low levels of proliferation.

Amiloride is known to display different pharmacological activities. A major alternative effect is the modulation of the alternative splicing of cancer-related genes, but the required concentration would be too high for clinical use (31, 32). In this study, the amiloride levels in the cell culture experiments was set at 100 μM, which is lower than that required for modulating gene splicing (31). In the animal model, we administered the lowest amiloride concentration by gavage (5 mg/kg/day) as previously reported (33). Although no study has reported on the effect of combining sorafenib treatment with amiloride, a recent study on the combination of sorafenib and hexamethylene amiloride (HMA; 524× amiloride activity), an amiloride analogue, has demonstrated its effectiveness in treating acute myeloid cells of leukemia (34). In addition, BS008, a new amiloride derivative that strongly modulates alternative splicing of multiple gene transcripts, has been reported to enhance the effect of sorafenib in Huh-7 hepatoma cells (32). Although the involvement of this derivative agent in uPA activity is unclear, the evidence suggests that the combination of sorafenib with analogous amiloride may be useful. Amiloride is a clinically well-tolerated diuretic that has few side-effects (30). We suggest that the clinically available amiloride may safely enhance the effect of sorafenib in part through inhibition of uPA activity.

Sorafenib is a unique small molecule that was originally developed as an inhibitor of Raf kinase and was later identified as targeting a broad range of signaling pathways (4, 35, 36). This broad targeting could mean that several potential non-Raf molecules could in turn be activated to counteract the sorafenib effect. Therefore, it is desirable to examine sorafenib resistance mechanisms from a novel angle, such as soluble-factor-mediated resistance.

In conclusion, we identified uPA as a potential target for sorafenib resistance in HCC cells. Combination treatment with uPA inhibitors or knockdown of uPA gene improved the effect of sorafenib, suggesting that uPA may be the key to overcoming drug resistance. Further studies are needed to confirm the safety and efficacy of uPA-based sorafenib combination therapy in HCC patients.

Conflicts of Interest

The Authors declare that they have no conflicts of interest regarding this study.

Authors' Contributions

MO conceived and provided the study design, MO and YM performed most of the experiments, all authors were involved in data interpretation, MO and YM wrote the manuscript, and TW and YK reviewed the manuscript. The final version of the manuscript was read and approved by all of the Authors.

References

1 El-Serag HB: Hepatocellular carcinoma. N Engl J Med *365(12)*: 1118-1127, 2011. PMID: 21992124. DOI: 10.1056/NEJMra1001683

2 Llovet JM, Burroughs A and Bruix J: Hepatocellular carcinoma. Lancet *362(9399)*: 1907-1917, 2003. PMID: 14667750. DOI: 10.1016/S0140-6736(03)14964-1

3 Doycheva I and Thuluvath PJ: Systemic therapy for advanced hepatocellular carcinoma: An update of a rapidly evolving field. J Clin Exp Hepatol *9(5)*: 588-596, 2019. PMID: 31695249. DOI: 10.1016/j.jceh.2019.07.012

4 Rimassa L and Worns MA: Navigating the new landscape of second-line treatment in advanced hepatocellular carcinoma. Liver Int *40(8)*: 1800-1811, 2020. PMID: 32432830. DOI: 10.1111/liv.14533

5 Wilhelm SM, Carter C, Tang L, Wilkie D, McNabola A, Rong H, Chen C, Zhang X, Vincent P, McHugh M, Cao Y, Shujath J, Gawlak S, Eveleigh D, Rowley B, Liu L, Adnane L, Lynch M, Auclair D, Taylor I, Gedrich R, Voznesensky A, Riedl B, Post LE, Bollag G and Trail PA: BAY 43-9006 exhibits broad spectrum oral antitumor activity and targets the RAF/MEK/ERK pathway and receptor tyrosine kinases involved in tumor progression and angiogenesis. Cancer Res *64(19)*: 7099-7109, 2004. PMID: 15466206. DOI: 10.1158/0008-5472.CAN-04-1443

6 Wilhelm SM, Adnane L, Newell P, Villanueva A, Llovet JM and Lynch M: Preclinical overview of sorafenib, a multikinase inhibitor that targets both Raf and VEGF and PDGF receptor tyrosine kinase signaling. Mol Cancer Ther *7(10)*: 3129-3140, 2008. PMID: 18852116. DOI: 10.1158/1535-7163.MCT-08-0013

7 Cheng AL, Kang YK, Chen Z, Tsao CJ, Qin S, Kim JS, Luo R, Feng J, Ye S, Yang TS, Xu J, Sun Y, Liang H, Liu J, Wang J, Tak WY, Pan H, Burock K, Zou J, Voliotis D and Guan Z: Efficacy and safety of sorafenib in patients in the asia-pacific region with advanced hepatocellular carcinoma: A phase iii randomised, double-blind, placebo-controlled trial. Lancet Oncol *10(1)*: 25-34, 2009. PMID: 19095497. DOI: 10.1016/S1470-2045(08)70285-7

8 Liu L, Chen H, Wang M, Zhao Y, Cai G, Qi X and Han G: Combination therapy of sorafenib and TACE for unresectable HCC: A systematic review and meta-analysis. PLoS One *9(3)*: e91124, 2014. PMID: 24651044. DOI: 10.1371/journal.pone.0091124

9 Lencioni R, Llovet JM, Han G, Tak WY, Yang J, Guglielmi A, Paik SW, Reig M, Kim DY, Chau GY, Luca A, Del Arbol LR, Leberre MA, Niu W, Nicholson K, Meinhardt G and Bruix J: Sorafenib or placebo plus TACE with doxorubicin-eluting beads for intermediate

stage HCC: The space trial. J Hepatol *64(5)*: 1090-1098, 2016. PMID: 26809111. DOI: 10.1016/j.jhep.2016.01.012

10 Goyal L, Zheng H, Abrams TA, Miksad R, Bullock AJ, Allen JN, Yurgelun MB, Clark JW, Kambadakone A, Muzikansky A, Knowles M, Galway A, Afflitto AJ, Dinicola CF, Regan E, Hato T, Mamessier E, Shigeta K, Jain RK, Duda DG and Zhu AX: A phase ii and biomarker study of sorafenib combined with modified folfox in patients with advanced hepatocellular carcinoma. Clin Cancer Res *25(1)*: 80-89, 2019. PMID: 30190369. DOI: 10.1158/1078-0432.CCR-18-0847

11 Niu L, Liu L, Yang S, Ren J, Lai PBS and Chen GG: New insights into sorafenib resistance in hepatocellular carcinoma: Responsible mechanisms and promising strategies. Biochim Biophys Acta Rev Cancer *1868(2)*: 564-570, 2017. PMID: 29054475. DOI: 10.1016/j.bbcan.2017.10.002

12 Tang W, Chen Z, Zhang W, Cheng Y, Zhang B, Wu F, Wang Q, Wang S, Rong D, Reiter FP, De Toni EN and Wang X: The mechanisms of sorafenib resistance in hepatocellular carcinoma: Theoretical basis and therapeutic aspects. Signal Transduct Target Ther *5(1)*: 87, 2020. PMID: 32532960. DOI: 10.1038/s41392-020-0187-x

13 Huynh H, Ngo VC, Koong HN, Poon D, Choo SP, Thng CH, Chow P, Ong HS, Chung A and Soo KC: Sorafenib and rapamycin induce growth suppression in mouse models of hepatocellular carcinoma. J Cell Mol Med *13(8B)*: 2673-2683, 2009. PMID: 19220580. DOI: 10.1111/j.1582-4934.2009.00692.x

14 Zhang R, Chen Z, Wu SS, Xu J, Kong LC and Wei P: Celastrol enhances the anti-liver cancer activity of sorafenib. Med Sci Monit *25*: 4068-4075, 2019. PMID: 31152143. DOI: 10.12659/MSM.914060

15 Gao Y, Fan X, Li N, Du C, Yang B, Qin W, Fu J, Markowitz GJ, Wang H, Ma J, Cheng S and Yang P: CCL22 signaling contributes to sorafenib resistance in hepatitis b virus-associated hepatocellular carcinoma. Pharmacol Res *157*: 104800, 2020. PMID: 32278046. DOI: 10.1016/j.phrs.2020.104800

16 Strumberg D, Richly H, Hilger RA, Schleucher N, Korfee S, Tewes M, Faghih M, Brendel E, Voliotis D, Haase CG, Schwartz B, Awada A, Voigtmann R, Scheulen ME and Seeber S: Phase i clinical and pharmacokinetic study of the novel raf kinase and vascular endothelial growth factor receptor inhibitor bay 43-9006 in patients with advanced refractory solid tumors. J Clin Oncol *23(5)*: 965-972, 2005. PMID: 15613696. DOI: 10.1200/JCO.2005.06.124

17 Labeur TA, Hofsink Q, Takkenberg RB, van Delden OM, Mathot RAA, Schinner R, Malfertheiner P, Amthauer H, Schutte K, Basu B, Kuhl C, Mayerle J, Ricke J and Klumpen HJ: The value of sorafenib trough levels in patients with advanced hepatocellular carcinoma - a substudy of the soramic trial. Acta Oncol *59(9)*: 1028-1035, 2020. PMID: 32366155. DOI: 10.1080/0284186X.2020.1759826

18 Salama R, Sadaie M, Hoare M and Narita M: Cellular senescence and its effector programs. Genes Dev *28(2)*: 99-114, 2014. PMID: 24449267. DOI: 10.1101/gad.235184.113

19 Krishnan A, Koski G and Mou X: Characterization of microcystin-induced apoptosis in HepG2 hepatoma cells. Toxicon *173*: 20-26, 2020. PMID: 31734250. DOI: 10.1016/j.toxicon.2019.11.003

20 Trojanowska M: ETS factors and regulation of the extracellular matrix. Oncogene *19(55)*: 6464-6471, 2000. PMID: 11175362. DOI: 10.1038/sj.onc.1204043

21 Gedaly R, Angulo P, Hundley J, Daily MF, Chen C, Koch A and Evers BM: Pi-103 and sorafenib inhibit hepatocellular carcinoma cell proliferation by blocking Ras/Raf/MAPK and PI3K/AKT/mTOR pathways. Anticancer Res *30(12)*: 4951-4958, 2010. PMID: 21187475.

22 Fujimaki S, Matsuda Y, Wakai T, Sanpei A, Kubota M, Takamura M, Yamagiwa S, Yano M, Ohkoshi S and Aoyagi Y: Blockade of ataxia telangiectasia mutated sensitizes hepatoma cell lines to sorafenib by interfering with Akt signaling. Cancer Lett *319(1)*: 98-108, 2012. PMID: 22265862. DOI: 10.1016/j.canlet.2011.12.043

23 Testa JE and Quigley JP: The role of urokinase-type plasminogen activator in aggressive tumor cell behavior. Cancer Metastasis Rev *9(4)*: 353-367, 1990. PMID: 2129023. DOI: 10.1007/BF00049524

24 Wang L, Zhang Y, Wang W, Zhu Y, Chen Y and Tian B: Gemcitabine treatment induces endoplasmic reticular (ER) stress and subsequently upregulates urokinase plasminogen activator (uPA) to block mitochondrial-dependent apoptosis in Panc-1 cancer stem-like cells (CSCs). PLoS One *12(8)*: e0184110, 2017. PMID: 28854261. DOI: 10.1371/journal.pone.0184110

25 Salvi A, Conde I, Abeni E, Arici B, Grossi I, Specchia C, Portolani N, Barlati S and De Petro G: Effects of miR-193a and sorafenib on hepatocellular carcinoma cells. Mol Cancer *12*: 162, 2013. PMID: 24330766. DOI: 10.1186/1476-4598-12-162

26 Gao XN, Lin J, Li YH, Gao L, Wang XR, Wang W, Kang HY, Yan GT, Wang LL and Yu L: MicroRNA-193a represses c-kit expression and functions as a methylation-silenced tumor suppressor in acute myeloid leukemia. Oncogene *30(31)*: 3416-3428, 2011. PMID: 21399664. DOI: 10.1038/onc.2011.62

27 Rose A, Grandoch M, vom Dorp F, Rubben H, Rosenkranz A, Fischer JW and Weber AA: Stimulatory effects of the multi-kinase inhibitor sorafenib on human bladder cancer cells. Br J Pharmacol *160(7)*: 1690-1698, 2010. PMID: 20649572. DOI: 10.1111/j.1476-5381.2010.00838.x

28 Wang Z, Wang M and Carr BI: Involvement of receptor tyrosine phosphatase dep-1 mediated PI3K-cofilin signaling pathway in sorafenib-induced cytoskeletal rearrangement in hepatoma cells. J Cell Physiol *224(2)*: 559-565, 2010. PMID: 20432459. DOI: 10.1002/jcp.22160

29 Alfano D, Ragno P, Stoppelli MP and Ridley AJ: RhoB regulates uPAR signalling. J Cell Sci *125(Pt 10)*: 2369-2380, 2012. PMID: 22366462. DOI: 10.1242/jcs.091579

30 Matthews H, Ranson M and Kelso MJ: Anti-tumour/metastasis effects of the potassium-sparing diuretic amiloride: An orally active anti-cancer drug waiting for its call-of-duty? Int J Cancer *129(9)*: 2051-2061, 2011. PMID: 21544803. DOI: 10.1002/ijc.26156

31 Chang WH, Liu TC, Yang WK, Lee CC, Lin YH, Chen TY and Chang JG: Amiloride modulates alternative splicing in leukemic cells and resensitizes Bcr-ABLT315I mutant cells to imatinib. Cancer Res *71(2)*: 383-392, 2011. PMID: 21224352. DOI: 10.1158/0008-5472.CAN-10-1037

32 Lee CC, Chang WH, Chang YS, Yang JM, Chang CS, Hsu KC, Chen YT, Liu TY, Chen YC, Lin SY, Wu YC and Chang JG: Alternative splicing in human cancer cells is modulated by the amiloride derivative 3,5-diamino-6-chloro-n-(n-(2,6-dichloro benzoyl)carbamimidoyl)pyrazine-2-carboxide. Mol Oncol *13(8)*: 1744-1762, 2019. PMID: 31152681. DOI: 10.1002/1878-0261.12524

33 Guan B, Hoque A and Xu X: Amiloride and guggulsterone suppression of esophageal cancer cell growth *in vitro* and in nude mouse xenografts. Front Biol (Beijing) *9(1)*: 75-81, 2014. PMID: 24999355. DOI: 10.1007/s11515-014-1289-z

34 Man CH, Lam SS, Sun MK, Chow HC, Gill H, Kwong YL and Leung AY: A novel tescalcin-sodium/hydrogen exchange axis underlying sorafenib resistance in FLT3-ITD$^+$ AML. Blood *123(16)*: 2530-2539, 2014. PMID: 24608976. DOI: 10.1182/blood-2013-07-512194

35 Yu C, Bruzek LM, Meng XW, Gores GJ, Carter CA, Kaufmann SH and Adjei AA: The role of Mcl-1 downregulation in the proapoptotic activity of the multikinase inhibitor BAY 43-9006. Oncogene *24(46)*: 6861-6869, 2005. PMID: 16007148. DOI: 10.1038/sj.onc.1208841

36 Coriat R, Nicco C, Chereau C, Mir O, Alexandre J, Ropert S, Weill B, Chaussade S, Goldwasser F and Batteux F: Sorafenib-induced hepatocellular carcinoma cell death depends on reactive oxygen species production *in vitro* and *in vivo*. Mol Cancer Ther *11(10)*: 2284-2293, 2012. PMID: 22902857. DOI: 10.1158/1535-7163.MCT-12-0093

Received December 11, 2020
Revised December 25, 2020
Accepted December 28, 2020